

Supporting Information

Construction of Light-Responsible Phase Chirality from Achiral Macrogelator

Yu-Jin Choi,¹ Won-Jin Yoon,¹ Minwook Park, Dong-Gue Kang, Geukcheon Bang, Jahyeon Koo, Seok-In Lim, Seohee Park, and Kwang-Un Jeong*

Polymer Materials Fusion Research Center & Department of Polymer-Nano Science and Technology, Chonbuk National University, Jeonju 54896, Republic of Korea

*E-mail: kujeong@jbnu.ac.kr

Synthetic procedures

Compound 1: To a stirred solution of 4-(2-(2-(2-((4'-(octyloxy)-[1,1'-biphenyl]-4-yl)oxy)ethoxy)ethoxy) ethoxy)bezoate (0.95 g, 1.64 mmol) in tetrahydrofuran and methanol (10 ml/ 8 ml) was added aqueous sodium hydroxide (ca. 10 M, 4.1 ml). The mixture was refluxed for 5 hours at 60 °C and then neutralized with an aqueous hydrochloric acid. The precipitate was filtered off and washed with water. The crude product was purified by re-precipitation with chloroform and ethanol and dried under vacuum to afford compound 1 as a yellow solid (Yield: 0.94g, 95 %). ¹H NMR, δH(400 MHz, CDCl₃): 0.89 (3 H, t, CH₃), 1.23-1.21 (10 H, m, CH₂), 1.80 (2 H, m, CH₂), 3.77 (4 H, t, OCH₂), 3.89 (4 H, m, OCH₂), 4.02 (2 H, t, OCH₂), 4.20 (4 H, m, OCH₂), 6.99 (6 H, m, ArH), 7.84 (4 H, q, ArH), 8.01 (2 H, d, ArH).

Compound 2: 1,4-phenylenediamine (1.868 g, 17.28 mmol), compound 1 (1.0 g, 1.73 mmol), and DPTS (4-(dimethylamino)pyridinium-4-toluenesulfonate, 0.254 g, 0.86 mmol) were added to a sealed round-bottomed flask containing a magnetic stirring bar in 50 mL, MC/THF solution and stirred at 0 °C for 30 min. DIPC (diisopropylcarbodiimide, 1.09 g, 8.64 mmol) was then dissolved into the mixture and the solution was stirred at 0 °C for 24 h. After reaction, 50 ml H₂O was poured into the solution and then extracted with MC (3 × 30 ml). The crude product subjected to column chromatography (silica, MC/THF = 4:1 (v/v)) to remove double substitute bisamide. After chromatography, products were re-precipitated from MeOH and filtered off to obtain compound as yellow powder (Yield: 0.85 g, 74 %). ¹H NMR, δH(400 MHz, CDCl₃): 0.89 (3 H, t, CH₃), 1.23-1.21 (10 H, m, CH₂), 1.80 (2 H, m, CH₂), 3.62 (2 H, s, CH₂), 3.77 (4 H, t, OCH₂), 3.89 (4 H, m, OCH₂), 4.02 (2 H, t, OCH₂), 4.20 (4 H, m, OCH₂), 6.68 (2 H, d, NH₂), 6.99 (6 H, m, ArH), 7.36 (2 H, d, ArH), 7.57 (1 H, s, NH), 7.84 (4 H, q, ArH), 8.01 (2 H, d, ArH).

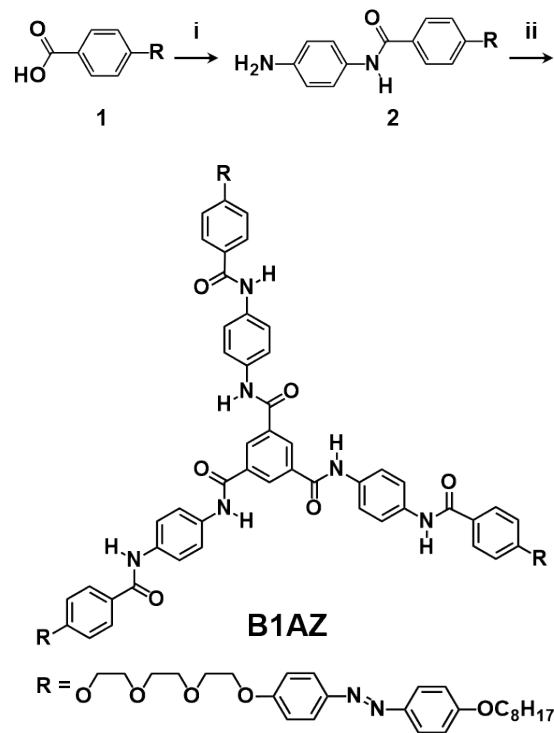


Fig. S1 Synthetic procedures of achiral B1AZ macrogelator.

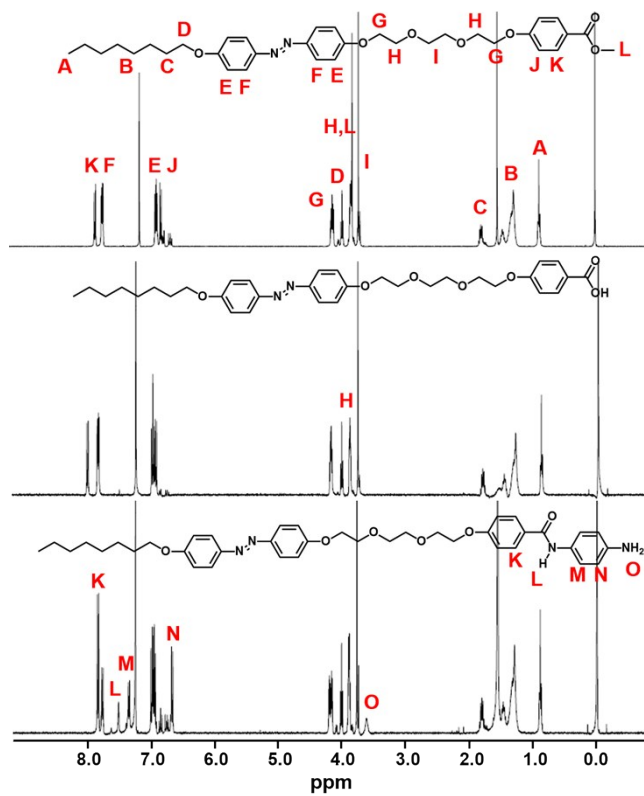


Fig. S2 ^1H NMR spectra of precursors of azobenzene molecular machine.

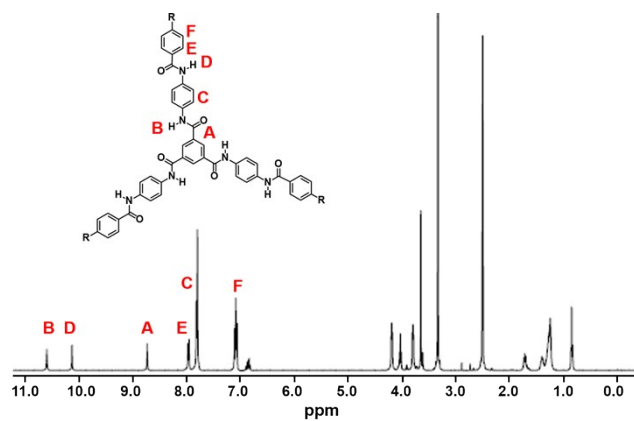


Fig. S3 ^1H NMR spectrum of achiral B1AZ macrogelator.

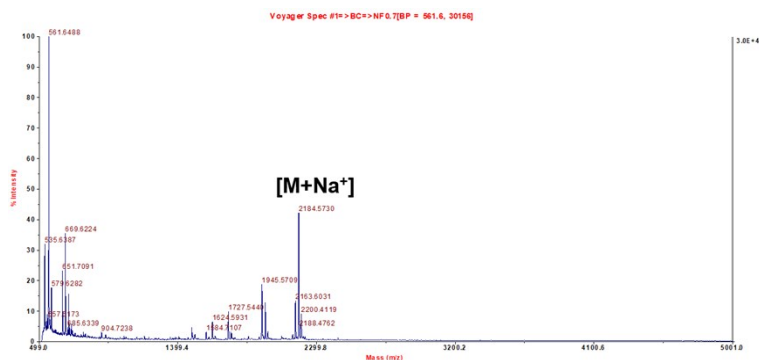


Fig. S4 MALDI-ToF spectrum of achiral B1AZ macrogelator.

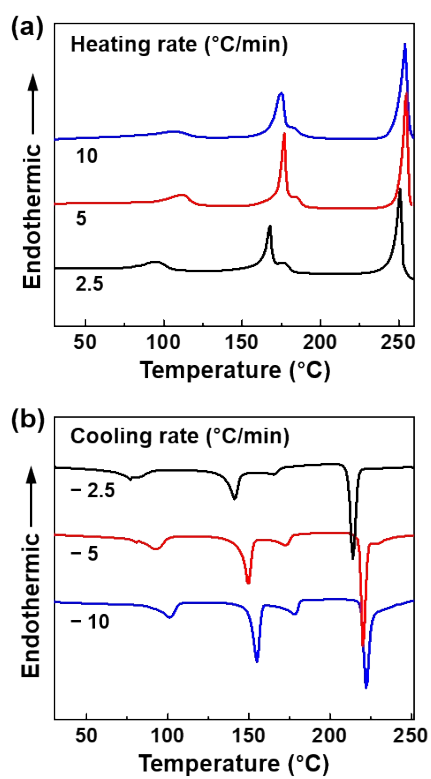


Fig. S5 DSC thermograms upon (a) heating and (b) subsequent cooling process at the different scanning rates from 2.5 to 10 °C min⁻¹.

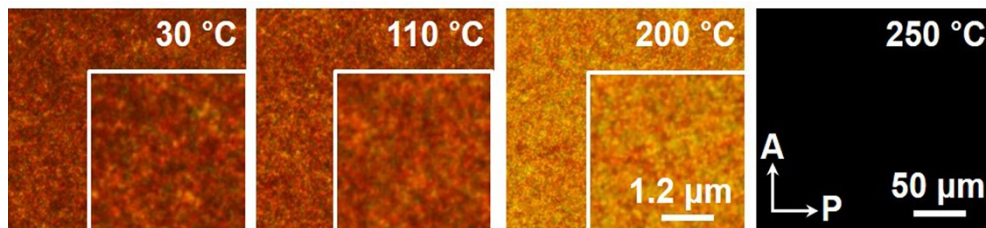


Fig. S6 POM images with enlarged image (insert) at different temperatures taken during the 2.5 °C min⁻¹ cooling process.

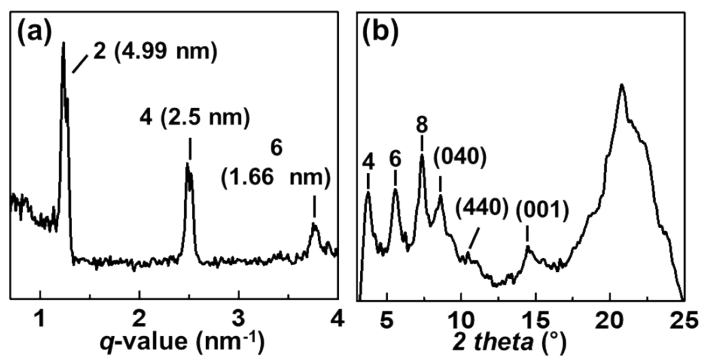


Fig. S7 (a) 1D SAXS and (b) 1D WAXD patterns of B1AZ powder at room temperature.

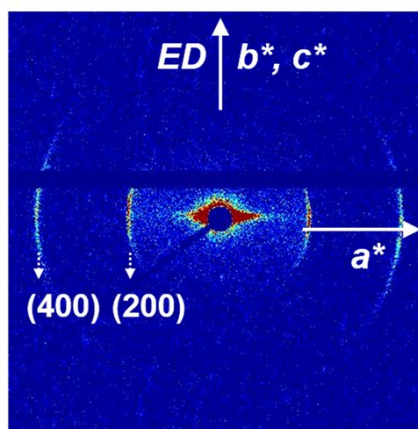


Fig. S8 2D SAXS pattern of the oriented B1AZ sample at room temperature.

Table S1 Experimental and calculated crystallographic parameters of lamello-columnar phase of BIAZ.

<i>(hkl)</i>	2θ (deg)		<i>d</i> -spacing (nm)	
	Expt ^a	Calc ^b	Expt ^a	Calc ^b
(040)	7.5	8.01	1.17	1.10
(070)	14.9	14.05	0.59	0.63
(001)	11.4	11.4	0.78	0.78
(002)	22.5	22.5	0.39	0.39
(200)	1.78	1.76	4.99	5
(400)	3.5	3.53	2.52	2.5
(440)	8.4	8.76	1.05	1.01
(600)	5.5	5.3	1.6	1.67
(800)	7.7	7.4	1.14	1.19
(1600)	13.4	13.9	0.66	0.63
(2000)	19	18.5	0.47	0.48

^a Experimental values observed in both WAXD. ^b The calculated data listed are based on the orthorhombic unit cell with $a = 10$ nm, $b = 4.41$ nm, $c = 0.78$ nm, $\alpha = \beta = \gamma = 90^\circ$.

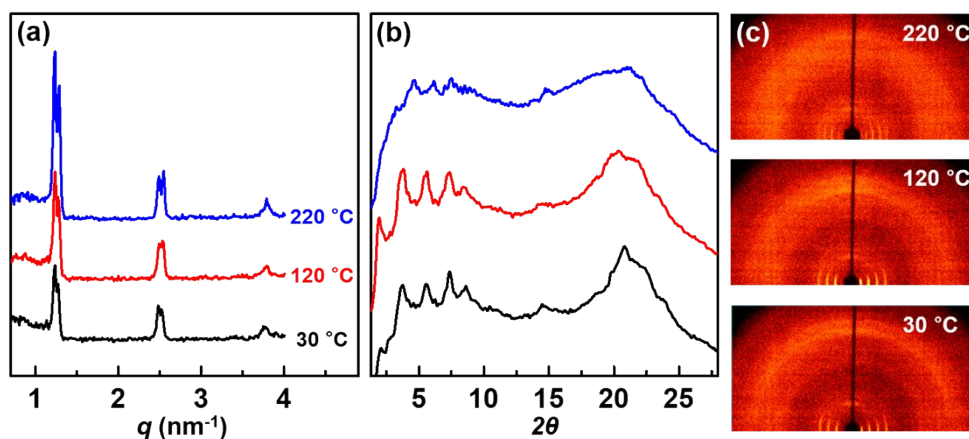


Fig. S9 Temperature-dependent (a) 1D SAXS, (b) 1D WAXD, and (c) 2D WAXD patterns of BIAZ. Here, the black, red, and blue line represent the status at 30 °C, 120 °C, and 220 °C.

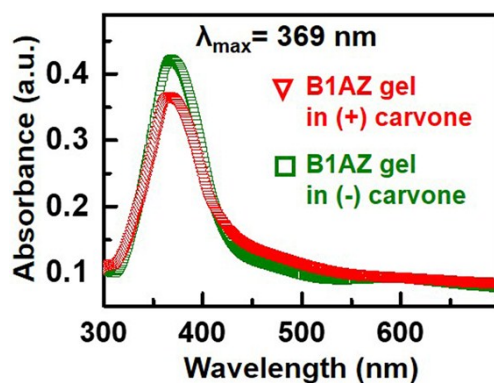


Fig. S10 UV-vis spectrum of B1AZ gels consisting (+), (-) carvones, respectively.

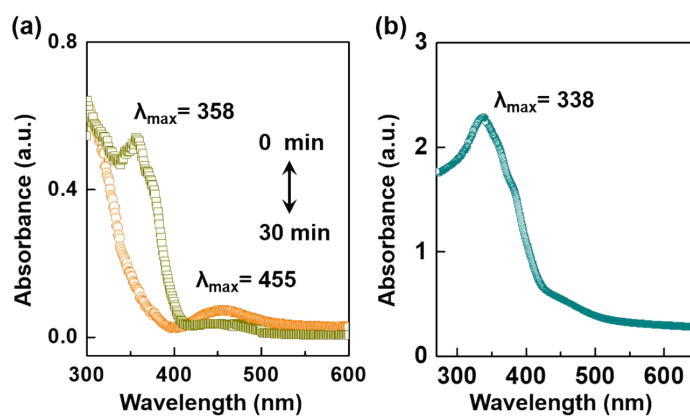


Fig. S11 UV-vis spectra of achiral B1AZ observed in (a) solution and (b) solid state, respectively. Here, reversible photo-isomerization upon UV (365 nm) and Vis (450 nm) exposure in THF solution are indicated in the Fig. S11(a).

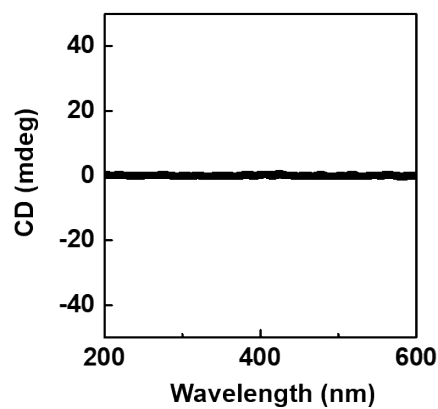


Fig. S12 CD spectrum of B1AZ powder at room temperature.

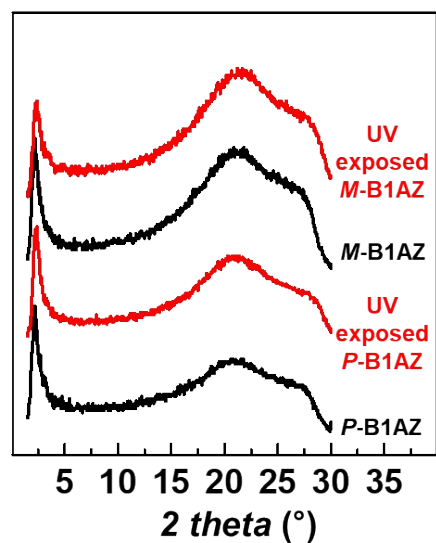


Fig. S13 (a) 1D WAXD patterns of (*P*), (*M*)-B1AZ and UV-exposed (*P*), (*M*)-B1AZ for 5 h, respectively.

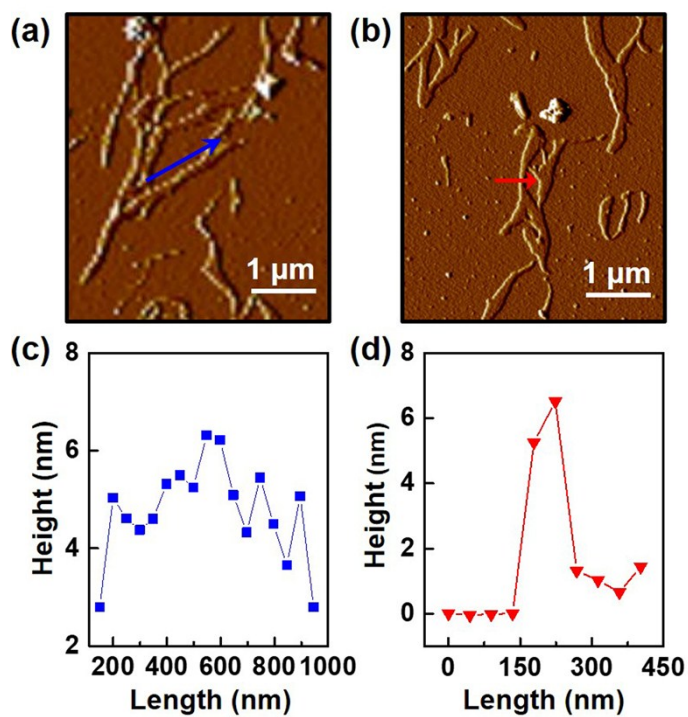


Fig. S14 (a) 2D AFM image of (*M*)-B1AZ xerogel and (b) subsequently UV exposed image for 5 h. Height profiles along the (c) elongated axis (blue line) and (d) short axis (red line) of helix.

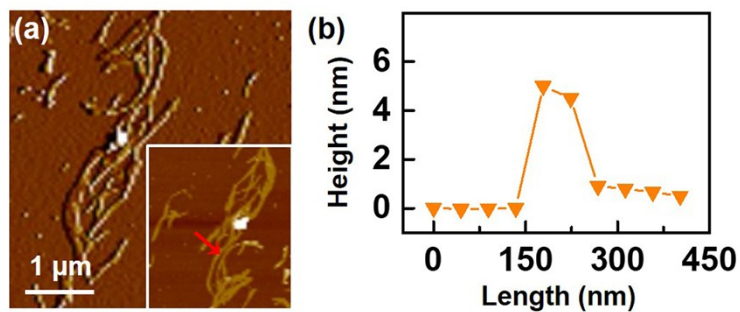


Fig. S15 (a) AFM image of (*P*)-B1AZ and UV-irradiated image (inset) with (b) that of height profile at room temperature.

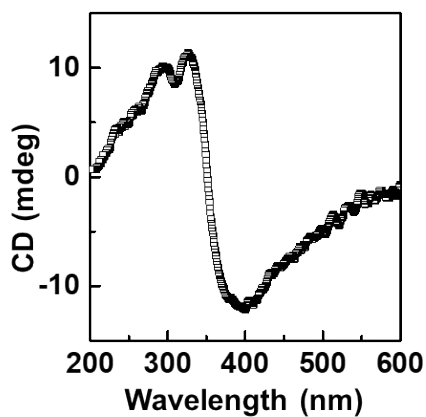


Fig. S16 CD spectrum of single helix obtained by (*M*)-B1AZ sol state at room temperature.

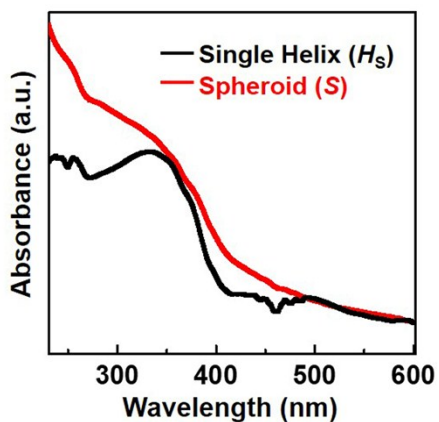


Fig. S17 UV spectra of single helix and spheroid of (*M*)-B1AZ extracted from the CD measurement at room temperature.

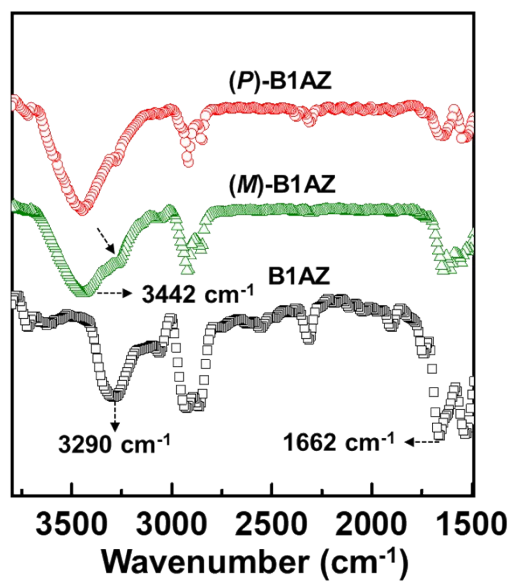


Fig. S18 FTIR spectra of pristine B1AZ powder, (*M*)-B1AZ, and (*P*) B1AZ at room temperature.